

Application of In-Situ Diagnostic Methods for the Study of SOFC Operational Behaviour

Günter Schiller, Wolfgang Bessler, Caroline Willich, K. Andreas Friedrich
Deutsches Zentrum für Luft- und Raumfahrt (DLR)
Institut für Technische Thermodynamik
Pfaffenwaldring 38-40, D-70569 Stuttgart, Germany
Tel.: +49-711-6862635
Fax: +49-711-6862747
guenter.schiller@dlr.de

Abstract

In order to optimise the operational behaviour of fuel cells and minimise cell degradation it is very helpful to use in-situ and ex-situ analytical methods. This paper gives an overview of in-situ diagnostic methods that are applied at DLR Stuttgart for the study of SOFCs. It includes spatially resolved measurements with an experimental segmented cell configuration where different techniques such as IV characteristics, impedance spectroscopy, gas chromatography and temperature measurement are involved. The investigation by means of segmented cells aims at the determination of local effects and the identification of critical operating conditions during technically relevant SOFC operation. Recently, a new test setup with transparent optical access has been built up allowing for microscopic observation of processes within the cell as well as for application of in-situ laser Raman spectroscopy to determine highly resolved concentrations of gas species along a flow channel. Examples of analytical studies by applying these diagnostic methods are presented and potentials and limitations of the different techniques are discussed.

Introduction

High electrical performance and long lifetime are key requirements that must be fulfilled for a successful introduction of fuel cells into the market. For achieving a high efficiency, a high fuel utilisation is required which means an electrochemical conversion of fuel into electricity as high as possible. This requirement, on the other hand, results in strong concentration gradients at the anode where the fuel is successively diluted by reaction products during the reaction process and, hence, in an inhomogeneous distribution of electrochemical performance and temperature. Inhomogeneous distributions of electrochemical and thermal properties such as local power density and local temperature might detrimentally affect both efficiency and long-term durability through thermo-mechanical stress and degradation phenomena induced by locally varying operating conditions. In order to optimise the operational behaviour of fuel cells and minimise cell degradation the application of advanced diagnostic methods by monitoring cell characteristics under real operating conditions can provide detailed information about the spatial distribution of the electrical, chemical and thermal cell properties. DLR has developed spatially resolved diagnostic techniques with a segmented cell arrangement where different techniques such as IV characteristics, impedance spectroscopy, gas chromatography and temperature measurement are involved [1, 2]. The segmented cell

setup allows a largely extended insight into fuel cell processes both for increasing the fundamental understanding and for optimising cell and flow field design. The obtained data can be used for mathematical modelling and model validation and for predicting physical, electrochemical and fluid mechanical properties [3, 4]. Recently, imaging techniques such as optical microscopy and Raman spectroscopy have been additionally adopted for in-situ observation of fuel cells. A test setup with transparent optical access allows for microscopic observation of relevant processes within the gas channels and the cell surface area as well as for the highly resolved determination of gas concentrations along the flow path of the fuel gas. The paper gives an overview of in-situ diagnostic methods applied at DLR Stuttgart for the determination of local effects and the identification of critical operating conditions during technically relevant SOFC operation. Exemplary results from experimental investigations are presented.

1. Experimental Details

The measurement setup for segmented cells as developed at DLR Stuttgart is shown schematically in Fig. 1. It allows for the integral and spatially resolved measurement of current density and voltage, the local and integral determination of impedance data, the local measurement of temperature and temperature distribution and the spatially resolved analysis of the fuel gas concentrations along the flow path. Square-shaped as well as rectangular cells with an area of 100 cm² are divided into 16 segments with an active area of each segment of 4.84 cm² and 3.78 cm², respectively. The cells are integrated in a metallic cell housing and sealed with glass seal. The metallic housing is also subdivided into 16 galvanically isolated segments. In order to determine the temperature at each segment, thermocouples are introduced in the metallic segments. Additionally, capillary tubes that correspond to the cathodic segments are integrated at the anode side at 16 measuring points to take samples of the anode gas to be analysed by gas chromatography. The setup is flexible with regard to the integration of different cell designs. Metal-supported cells (MSC), as they are developed and fabricated in house according to the DLR spray concept [5], as well as electrolyte-supported cells (ESC) and anode-supported cells (ASC) can be characterised. With MSC and ASC, only the cathode is segmented, whereas ESCs are segmented on both the anode and the cathode side. For the contact of the electrodes Ni and Pt meshes were used. More details on the measurement system are given in [2].

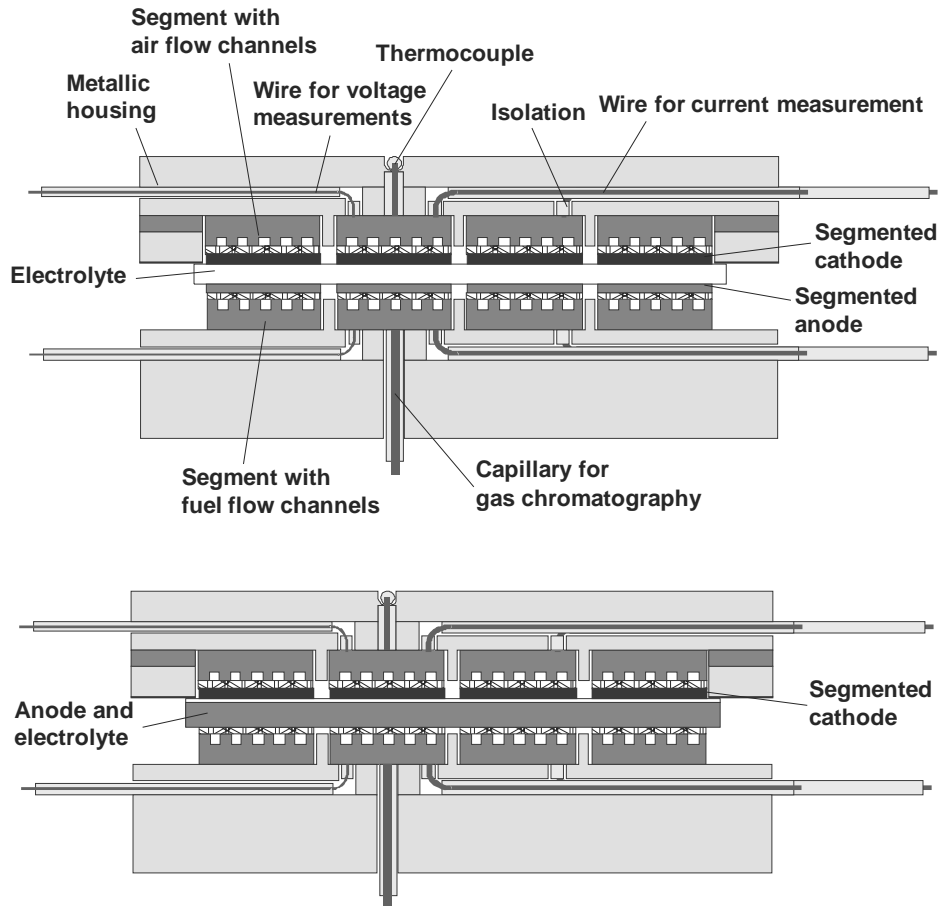


Fig. 1: Setup of measurement system for the characterisation of segmented cells:
 (a) Housing with anode and cathode segmentation used for ESC cells
 (b) Housing with cathode segmentation used for MSC and ASC cells

2. Results

The measuring system described has been applied to locally characterise SOFCs with the segmented cell arrangement. Three examples are given to demonstrate the potential of this spatially resolved measuring technique.

Power density distribution of a metal-supported cell (MSC)

As a first example the power density distribution over the 16 segments, each 4.6 cm^2 wide, of a plasma sprayed metal-supported cell ($100 \times 100 \text{ mm}^2$) is shown in Fig. 2 for an operating temperature of $800 \text{ }^\circ\text{C}$ [6]. The gas flow rates are $12.5 \text{ sccm/cm}^2 \text{ H}_2$, $12.5 \text{ sccm/cm}^2 \text{ N}_2$ as fuel and 80 sccm/cm^2 air as oxidant. The current density distribution varies tremendously over the cell. Maximum differences of 116.6 mW/cm^2 could be identified in Fig. 2. The worst segment reaches only 23.6 % of the power density of the best segment. The average power density of the cell was 125.6 mW/cm^2 at 0.7 V . In some segments (e.g. segment 4 and 16) a significant lower power density is observed probably due to a glass sealing failure. There is a slight increase of the power density of about 15.1 % in average over all segments from air inlet to air outlet. The main effect could be attributed to the inhomogeneous gas distribution at the inlet and to the sealing. The

differences in the electrochemical behaviour are also caused by local water production as a result of the slightly permeable electrolyte. It could be seen by local impedance spectroscopy that the current distribution is in good agreement with the local resistances.

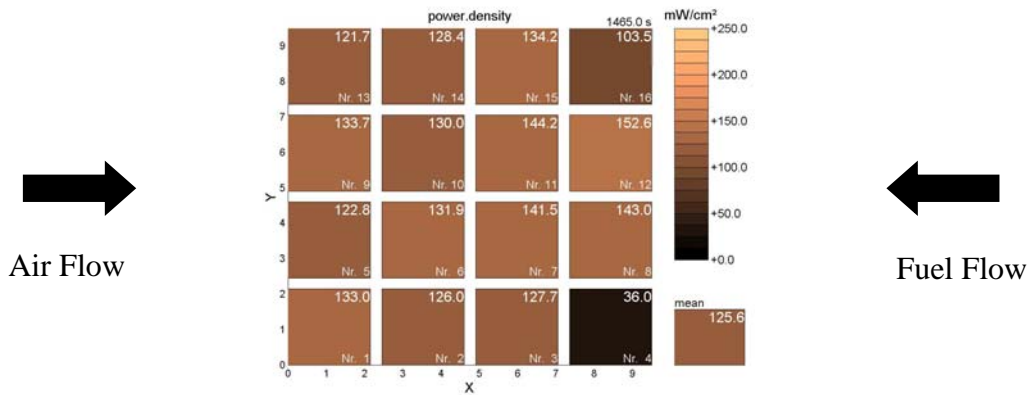


Fig. 2: Power density distribution of a plasma sprayed cell with an average cell voltage of 0.7 V

The local temperatures (Fig. 3) directly affect the ohmic resistances and should therefore be taken into account. The experiments revealed that the anode overpotential at an overall cell voltage of 0.7 V with the selected gas supply is very small and can be neglected without major error. As a consequence, the overpotential is mainly related to the cathode and further cell improvement should concentrate on improving performance of the oxygen reduction reaction. The results obtained by these measurements show a variation of the behaviour of the cell along the flow path. Current density, impedance and temperature can be associated with the observed effects. The obtained data can be used to avoid critical temperature gradients during operation and also to optimise functional layers to homogenise current density and heat production especially in a fuel cell stack.

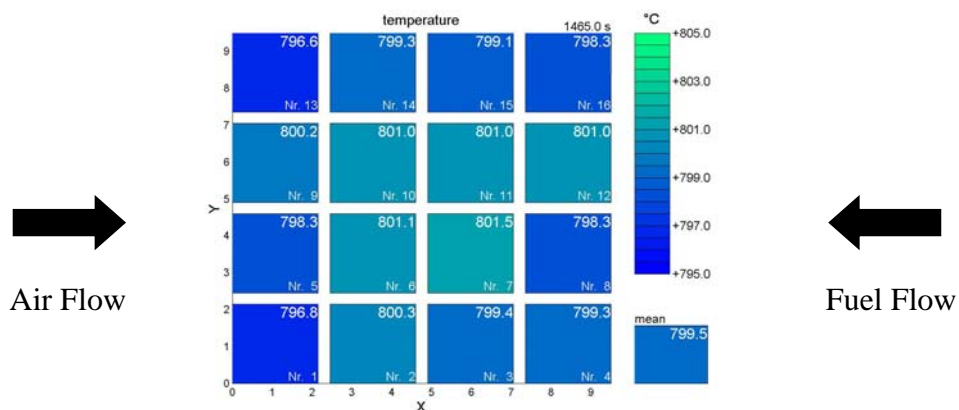


Fig. 3: Temperature distribution of a plasma sprayed cell with an average cell voltage of 0.7 V

Investigation of an anode-supported cell (ASC) with high fuel utilisation

A segmented anode-supported cell (ASC) containing a 540 μm thick NiO/YSZ anode with a thin anode functional layer, a 7 μm thick 8YSZ electrolyte, a 7 μm thick YDC interlayer and a 30 μm thick LSCF cathode was operated under a condition with high fuel utilisation. The anode was fed with 33 % H_2 , 1 % H_2O and 66 % N_2 . This condition was chosen in order to simulate nitrogen-rich reformat gas. The cathode was fed with air in counter-flow operation.

The measured two-dimensional distribution of power density at 800 $^\circ\text{C}$ in the 16 segments is shown in Fig. 4 for an average power density of 460 mW/cm^2 . The fuel utilisation at this condition is 80 %. The cell performance is strongly inhomogeneous, with the power density systematically decreasing from fuel inlet (left side of Fig. 4) to fuel outlet (right side of Fig. 4). It will be shown below that this decrease is due to fuel depletion along the flow path. Moreover, there is a notable difference for the four segment rows (upper row to lower row in Figure 4). This difference may be due to sealing issues or inhomogeneous gas supply to the gas channels. Further segment-to-segment scattering is likely due to a variation in contact resistance which may also lead to systematic row-to-row variations when the contact pressure is inhomogeneous. For comparison with the model (which represents the behaviour along one single channel), the row with segments 9-12 was chosen.

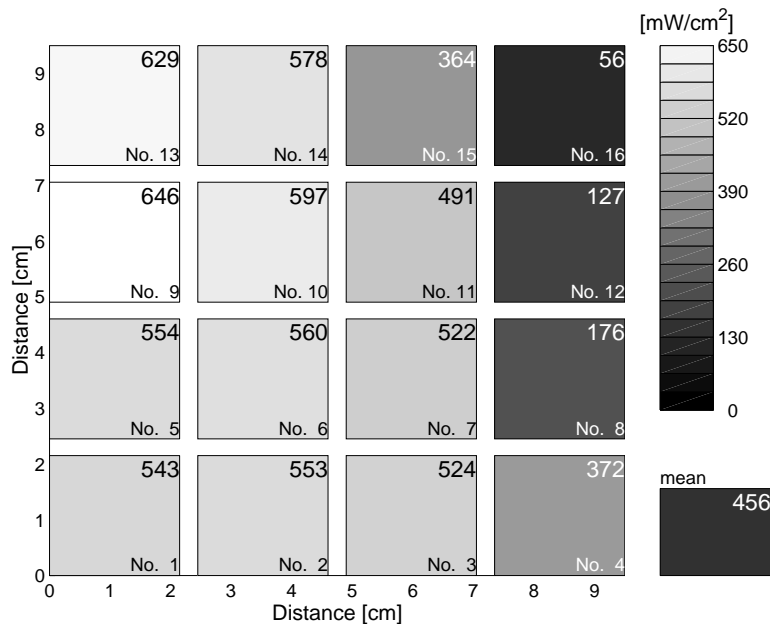


Fig. 4: Measured two-dimensional distribution of power density over the 16 segments under operating conditions with high fuel utilisation (counter-flow operation; anode: 33 % H_2 , 1 % H_2O , 66 % N_2 in H_2 , 1.1 m/s inflow velocity; cathode: air, 5.2 m/s inflow velocity; $T = 800$ $^\circ\text{C}$) at an average cell voltage of 0.59 V. The fuel inlet is on the left side, the air inlet at the right side.

Experimental and simulated global and local current-voltage characteristics for segments 9-12 are shown in Fig. 5. Simulations were performed using a 2D model along one representative channel and through the thickness of the MEA. This detailed 1D+1D elementary kinetic electrochemical model represents one single channel of the

experimental setup. One-dimensional channel flow (x dimension) is described using the Navier-Stokes conservation equations (continuity, species, momentum), corresponding essentially to a plug-flow model with axial diffusion. One-dimensional mass transport through the membrane-electrode assembly (MEA) (y dimension) is described by coupled Fickian/Knudsen diffusion and Darcy flow. Charge transport in the solid electrolyte and the electrolyte phase of the composite electrodes is described in two dimensions using Ohm's law. Details about the used model are described in [3].

The global IV-curve (Fig. 5a) shows a typical shape with a parabolic behaviour at low currents, linear behaviour at intermediate currents, and a limiting current density of ~ 0.8 A/cm² at high currents. The maximum power density ($P_{\max} = 470$ mW/cm²) is observed at a global cell voltage of 0.70 V. Local IV-curves for segments 9-12 are represented by plotting local segment voltage versus local segment current (Fig. 5b). The local behaviour shows a considerable variation of current density for different cell segments. At high polarisation, segments 11 and 12 that are located close to the fuel outlet show a particularly interesting behaviour: the current decreases while at the same time the segment voltage strongly decreases. This "inverse" behaviour is due to strong fuel depletion. At the same time, the current density of segment 9 that is located at the fuel inlet continues to increase. There is excellent quantitative agreement between model and experiment for both the local and the global behaviour.

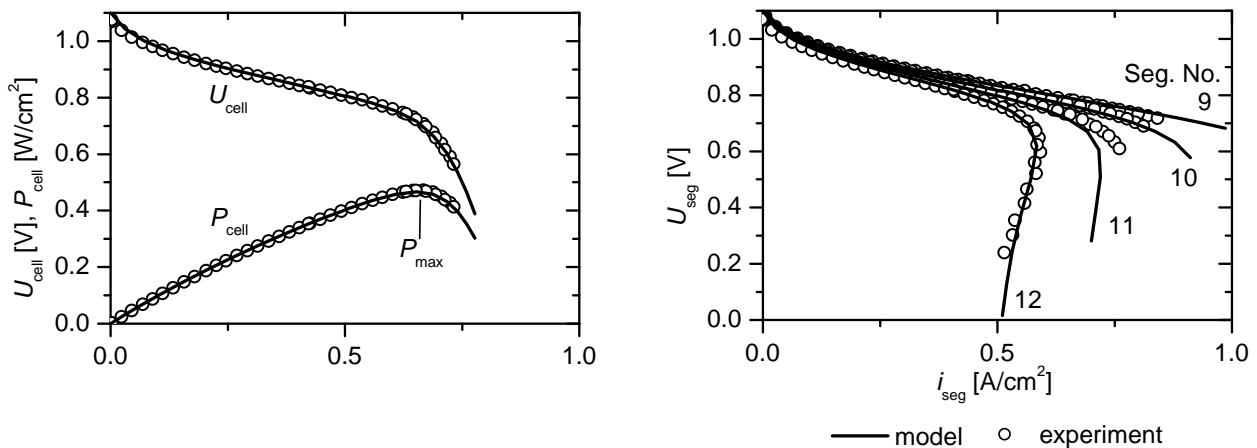


Fig. 5: Experimental and simulated polarisation behaviour for the segmented cell using the 2D model under operating conditions with high fuel utilisation (counter-flow operation; anode: 33 % H₂, 1 % H₂O, 66 % N₂ in H₂, 1.1 m/s inflow velocity; cathode: air, 5.2 m/s inflow velocity; T = 800 °C). (a) Global current-voltage curves, (b) local segment voltage versus local segment current. The numbers indicate the segments, where segment 9 is the first in flow direction of the fuel gas.

Operation of an anode-supported cell (ASC) with reformat as fuel gas

This example covers the operation of an anode-supported cell with a reformat composition as the fuel gas and the electrochemical reaction of the fuel gas components along the flow path [7]. A spatially resolved measurement along the flow path of the fuel with a realistic reformat composition (54.9 % N₂, 16.7 % H₂, 16.5 % CO, 6.6 % CH₄, 2.2 % CO₂, and 3.2 % H₂O) was performed to investigate the processes taking place in more

detail. The influence of the area-specific load on the power density and the fuel utilisation at operation of a segmented ASC cell (counter flow) along a row of segments (segment 9-12) with fuel inlet at segment 9 is shown in Fig. 6. The results in Fig. 6 reveal an excellent conversion of CO- and CH₄-containing fuel gas with 78.1 % at 400 mA/cm² and with 83.9 % at 435 mA/cm² at the fuel exit. At a current density between 0 and 200 mA/cm² the power density decreases only slightly along the flow path, but at a load of 400 mA/cm² a quite significant and strong reduction of power density at the fuel exit (segment 12) was observed. This behaviour is even more pronounced at a further increased current density of 435 mA/cm² of the total cell; segment 12 now shows a very low power density. It seems that the increasing conversion rate at the segments 9–11 causes performance reduction at segment 12 which could result in critical conditions and hence enhanced corrosion at the fuel exit.

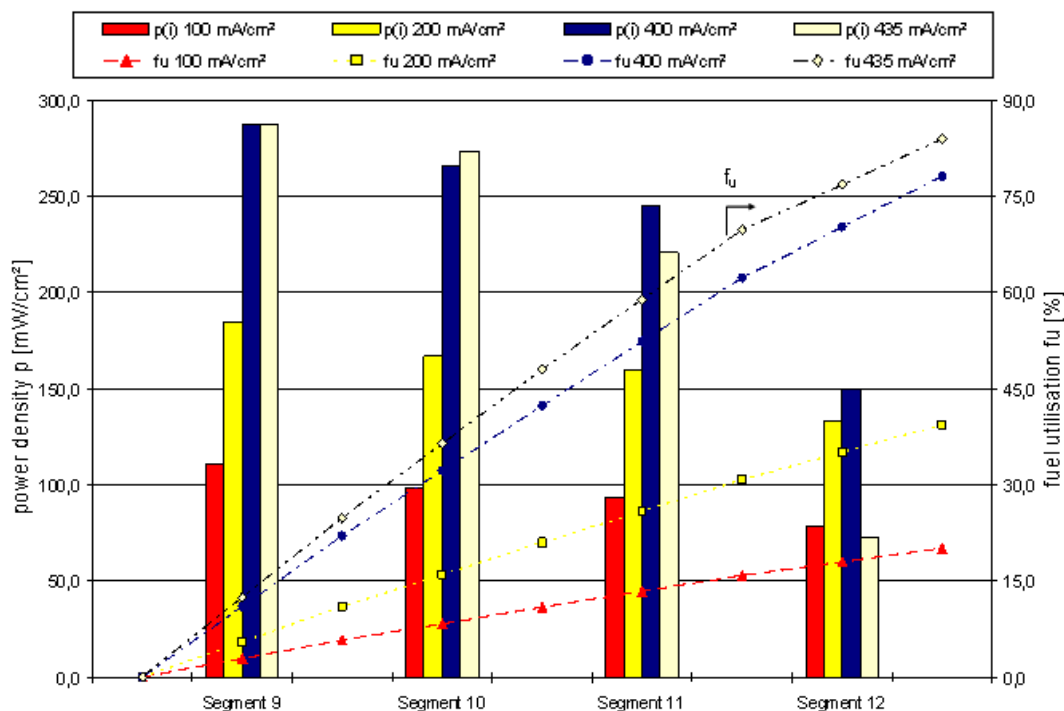


Fig. 6: Comparison of power density and fuel utilisation along the flow path during variation of the area-specific load of an ASC cell (active area: 73.96 cm²) during operation with reformat gas; counter-flow mode, fuel gas inlet at segment 9, fuel gas outlet at segment 12; current density equivalent: 0.552 A/cm², air flow rate: 0.02 slpm/cm²

In order to determine how the internal reforming of CH₄ which is a component of the reformat takes place, segments 9-12 were investigated at different current densities by means of gas chromatography measurements. These measurements showed clearly how the internal reforming of CH₄ increases with increasing current density. The increase of current density from 0 to 435 mA/cm² results in a higher conversion of H₂ to H₂O and CO to CO₂. A higher water content favours the shift and hence the reforming reaction. At 0 mA/cm² and 100 mA/cm² the water content drops at the segments 10 and 11 to almost 0%. The resulting diminished CO₂ and enhanced CO amount favours the Boudouard reaction and hence the carbon formation. With increasing current density above 100

mA/cm^2 the water content also increases continuously along the flow path thus avoiding critical conditions for the cell. At 200 mA/cm^2 methane is almost completely converted in the cell. With higher current density methane conversion is enhanced in direction of the fuel inlet. Due to the reforming of methane the hydrogen content at first increases at the fuel inlet at all current densities. At lower current densities and hence low conversion rates the hydrogen content is high whereas it decreases steadily at high current densities. The fuel utilisations calculated from the current densities correlate very well with the measured gas concentrations in the off-gas of the cell. Due to the higher formed hydrogen content during reforming and the low content of CO_2 compared to H_2O in the off-gas it is concluded that the oxidation of H_2 is favoured compared to CO oxidation. The changes of CO , H_2 and CH_4 in the balance of the components indicate a ratio of the reaction of H_2/CO of approximately 1.4. More details on the investigation of internal reforming of CH_4 are reported in [7].

3. Raman Spectroscopy and Optical Microscopy

The measurement setup for segmented cells described allows for the determination of gas concentrations by taking gas samples through tubes in the middle of each segment on the anode side and subsequent analysis by gas chromatography. A much higher spatial resolution along the anode gas channel can be achieved by applying one-dimensional laser Raman spectroscopy. This optical technique can be applied for measuring in-situ the number densities of several molecular species simultaneously, thus enabling the determination of the composition and concentration of relevant gaseous species (H_2 , H_2O , CH_4 , CO , CO_2 , N_2) within the flow channel of the anode with high spatial and temporal resolution. Solid-state Raman spectroscopy has been applied for studying SOFC processes ex-situ [8-11] but these studies were mainly devoted to the measurement of local temperature and mapping out of phase stability of solid electrode surfaces by monitoring the temporal variation of the oxidation state of materials. In our approach we apply in-situ gas-phase Raman spectroscopy of species concentrations and temperature during SOFC operation with technically relevant operating conditions.

In order to realise such measurements a new SOFC test rig has been built up which gives an optical access to the flow field of a SOFC cell setup through transparent windows in the furnace made of quartz glass as well as using a transparent anode flow field also entirely consisting of quartz glass. Because of the low quantum efficiency of the Raman scattering process, high laser pulse energies are indispensable. The laser system to be used for the Raman experiments at DLR consists of three double-pulse Nd:YAG lasers, frequency-doubled to 532 nm with $6 \times 300 \text{ mJ}$ pulse energy, 7 ns pulse duration and 10 Hz pulse repetition rate. The scattered light is collected at 90° with a large apochromatic lens system that relays the focal region of the laser beam onto the entrance slit of a grating spectrograph. The spectrally dispersed image of the beam is captured by a CCD camera. The objective of the experiments which will start in mid 2010 is the spatially resolved study of reactions taking place at the anode during SOFC operation under different operating conditions (variation of fuel gases including reformate compositions, temperature, fuel utilisation) and the comparison with results obtained from electrochemical impedance spectroscopy. The setup also enables optical microscopy through the transparent optical access to the cell by means of a long-distance microscope and a CCD camera in order to image the electrode surface with high spatial and temporal resolution. It is intended to investigate in this way coke formation and carbon and sulphur poisoning. The setup with the furnace and the microscope is shown in Fig. 7. By applying these new techniques for

in-situ observation of processes occurring during SOFC operation additional information and insight is expected for a better understanding of reactions and processes taking place under operational conditions.

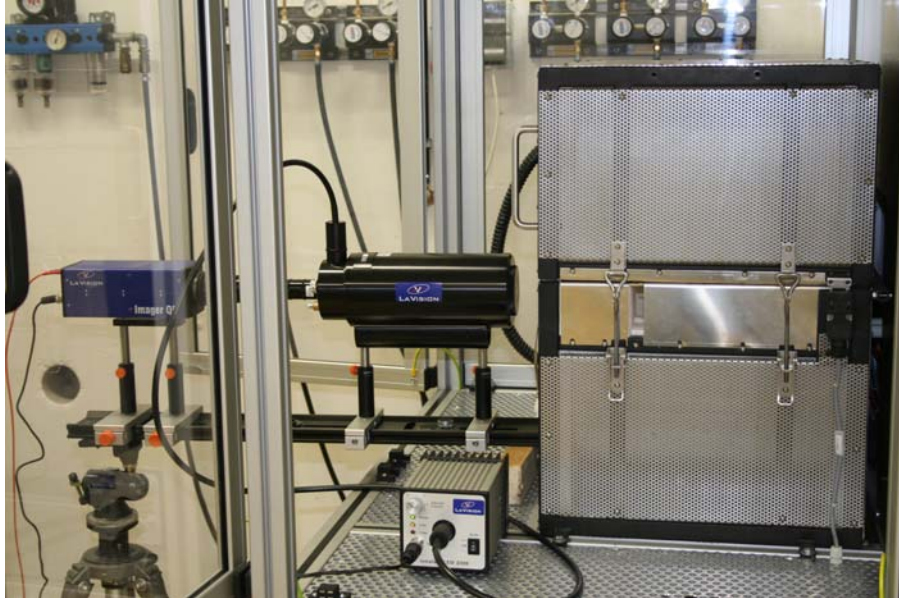


Fig. 7: Setup for in-situ optical microscopy with furnace, long-distance microscope and CCD camera

Conclusion

The spatially resolved diagnostic techniques with a segmented cell arrangement involving IV characteristics, impedance spectroscopy, gas chromatography and temperature measurement which were developed at DLR Stuttgart allow for a largely extended insight into fuel cell processes both for increasing the fundamental understanding and for optimising cell and flow field design. The obtained data can be used for mathematical modelling and simulation of fuel cell processes and local effects and critical operating conditions during technically relevant operation can be identified. The potential of this analytical method was demonstrated with 3 exemplary investigations with MSC and ASC cells. The identification of locally critical operating conditions due to strong gradients of gas concentrations and current density is particularly important at operation with high fuel utilisation. An experimental setup for the application of gas-phase Raman spectroscopy as well as optical microscopy by means of an optical access to the cell which is currently being built up might complement the existing diagnostic techniques and provide further information for the understanding of cell reactions and processes.

References

- [1] Patrick Metzger, Ortsaufgelöste Charakterisierung von Festelektrolyt-Brennstoffzellen (SOFC) durch Messung betriebsrelevanter Größen entlang des Strömungswegs, PhD Thesis, Universität Stuttgart, 2010
- [2] Patrick Metzger, K. Andreas Friedrich, Hans Müller-Steinhagen, Günter Schiller, SOFC Characteristics along the Flow Path, *Solid State Ionics* 177, 2045-2051, 2006
- [3] Wolfgang G. Bessler, Stefan Gewies, Caroline Willich, Günter Schiller, K. Andreas Friedrich, Spatial Distribution of Electrochemical Performance in a Segmented SOFC: A Combined Modeling and Experimental Study, *Fuel Cells*, in press, 2010
- [4] Günter Schiller, Wolfgang G. Bessler, K. Andreas Friedrich, Stefan Gewies, Caroline Willich, Spatially Resolved Performance in a Segmented Planar SOFC, *ECS Transactions* 17 (1), 79-87, 2009
- [5] Günter Schiller, Rudolf Henne, Michael Lang, Matthias Müller, Development of Solid Oxide Fuel Cells by Applying DC and RF Plasma Deposition Technologies, *Fuel Cells* 4 (1-2), 56-61, 2004
- [6] Patrick Metzger, K. Andreas Friedrich, Günter Schiller, Hans Müller-Steinhagen, Investigation of Locally Resolved SOFC Characteristics along the Flow Path, *ECS Transactions* 7 (1), 1841-1847, 2007
- [7] Patrick Metzger, K. Andreas Friedrich, Günter Schiller, Caroline Willich, Spatially Resolved Measuring Technique for SOFC, *Journal of Fuel Cell Science and Technology* 6 (2), 021304-1 - 021304-4, 2009
- [8] R. C. Maher, L. F. Cohen, P. Lohsoontorn, D. J. L. Brett, N. P. Brandon, Raman Spectroscopy as a Probe for Temperature and Oxidation State for Gadolinium-Doped Ceria Used in Solid Oxide Fuel Cells, *J. Phys. Chem. A* 112, 1497-1501, 2008
- [9] Michael P. Pomfret, Jeffrey C. Owrutsky, Robert A. Walker, High Temperature Raman Spectroscopy of Solid Oxide Fuel Cell Materials and Processes, *J. Phys. Chem. B* 110 (35), 17305-17308, 2006
- [10] Michael P. Pomfret, Jeffrey C. Owrutsky, Robert A. Walker, In Situ Studies of Fuel Oxidation in Solid Oxide Fuel Cells, *Anal. Chem.* 79 (6), 2367-2372, 2007
- [11] Zhe Cheng, Meilin Liu, Characterization of Sulphur Poisoning of Ni-YSZ Anodes for Solid Oxide Fuel Cells Using In Situ Microspectroscopy, *Solid State Ionics* 178 (13-14), 925-935, 2007